PS-InSAR based surface subsidence analysis in Changchun metropolitan area

He WANG[1]，Jiuchang MAO[2]，Shijun ZHAO[2]，Xinguo NING[3]，Qiong WU[1,*]

[1]College of Geo-exploration Science and Technology，Jilin University，Changchun 130026，China
[2]China Water Northeastern Investigation，Design&Research Co. Ltd，Changchun 130062, China
[3]Changchun Institute of Surveying and Mapping，Changchun 130021, China

Abstract The monitoring of urban land surface subsidence is the main task of urban disaster prevention and mitigation. In this paper, the land surface subsidence process in Changchun metropolitan area is calculated based on PS-InSAR technology by using the SLC data of Sentinel-1B with 50 scenes within the metropolitan area of Changchun from 2016 to 2020. The results show that the metropolitan surface of Changchun is basically in a stable state, the main settlement is located in the southeast of the metropolitan around the Century Square, the maximum settlement rate is 20.45mm/a, the average settlement rate is 2.98mm/a, the correlation coefficient between the settlement results calculated by PS-InSAR and the second-class leveling verification results reaches 0.67, which indicates that the regional settlement results calculated by PS-InSAR have high reliability. The subsidence area is dominated by the geological structure of the Mesozoic Cretaceous Yaojia Formation, with many intercalations of fine silty sand rocks and locally containing medium-coarse gravel sandstone. The overall structural stability is poor, which may be the main reason for subsidence in this area.

1 Introduce

Urban surface subsidence has the characteristics of slow formation, long duration, and irreversibility [1]. There are many reasons for the settlement, including unstable urban geological structure, urban construction, and over-exploitation of groundwater [2-5]. Large-scale urban ground subsidence may cause foundation collapse, underground pipeline damage and road damage [6]. Therefore, monitoring urban surface settlement is of great significance to urban disaster forecasting and urban maintenance.

Leveling measurement and global navigation satellite system (GNSS) measurement are the main ground surface monitoring methods for land subsidence, both of which can achieve millimeter-level measurement accuracy in urban areas. However, these two methods have high operating costs and long operating times, and can only be obtained. The settlement value of point-like and linear areas has low spatial resolution [7]. Synthetic Aperture Radar Interferometry (InSAR) has the characteristics of large monitoring range, low cost, high spatial resolution, and unaffected by climatic conditions [8-10]. Conventional synthetic aperture radar differential interferometry is susceptible to spatial decoherence, time decoherence, and atmospheric delay phase, and has certain limitations in application [11]. PS-InSAR recognizes permanent scatterers based on the time series of SAR images covering the same area and the amplitude dispersion index threshold method, which can maintain the scattering characteristics on long-term series and is almost free from the influence of time-space miscorrelation, which overcomes the differential synthetic aperture radar Insufficiency [12], it can monitor the long-term series of regional settlement processes with millimeter-level accuracy [13-14]. Sentinel, as free radar data, is widely used in urban land surface settlement monitoring. It has a good monitoring effect in the vertical direction of the area, and can reach a monitoring accuracy of 8mm. This article uses Sentinel-1B SLC data, based on PS-InSAR technology to monitor the surface settlement process in Changchun City from 2016 to 2020, identifies the main settlement areas and analyzes the main factors that occur.

2 Data and methods

2.1. Data sources

This article uses SLC data of 50 scenes of Sentinel-1B in the urban area of Changchun from October 2016 to December 2020, IW mode, VV polarization method, one scene is taken every month, and the DEM is SRTM-1 data with a resolution of 30m. , The accurate orbit ephemeris data comes from the Alaska radar data download network, and the ground verification data is the second-class level monitoring data in the urban area of Changchun City in November 2019 and September 2020.

* Corresponding author: Wuqiong@jlu.edu.cn

2.2. Calculation method

PS-InSAR extracts the phase of the PS point after differential interference processing for modeling and calculation. After subtracting the error components in the differential interferogram, the residual phase diagram is obtained, and the time-space filtering method is used to recover the residual phase time series, and various error phases are separated. Finally, the overall deformation is superimposed to obtain the deformation time series at each PS point.

When two adjacent PS points are modeled by neighborhood difference, the phase difference between them in the i-th interferogram is:

$$\Delta\phi_i(x_l,y_l,;x_p,y_p;T_i)=\frac{4\pi}{\lambda R sin\theta}B_i^{\perp}\Delta\varepsilon(x_l,y_l,;x_p,y_p)$$
$$+\Delta\varphi_i^{res}(x_l,y_l,;x_p,y_p;T_i)+\frac{4\pi}{\lambda}T_i\Delta_v(x_l,y_l,;x_p,y_p) \quad (1)$$

Where $B_i^{\perp}$ and T_i are the spatial vertical baseline and time baseline of the interference pair, respectively; λ, R and θ are the wavelength, the distance from the sensor to the target and the radar incident angle, respectively; $\Delta\varepsilon(x_l,y_l,;x_p,y_p)$, $\Delta\varphi_i^{res}(x_l,y_l,;x_p,y_p;T_i)$, and $\Delta_v(x_l,y_l,;x_p,y_p)$ are the elevation error and residual phase increment, respectively And LOS direction deformation rate increment.

Under the condition of $|\Delta\varphi_i^{res}|<\pi$, maximize the following objective function to find the solutions of $\Delta\varepsilon$ and Δ_v.

$$\gamma=\left|\frac{1}{M}\sum_{(i=1)}^{M}(cos\Delta\omega_i+i\,sin\Delta\omega_i)\right|=max \quad (2)$$

In the formula, γ is the model coherence coefficient between adjacent PS points; $i=\sqrt{-1}$; $\Delta\omega_i$ is the difference between the observed value and the fitted value, namely

$$\Delta\omega_i=\Delta\phi_i-\frac{4\pi}{\lambda R sin\theta}B_i^{\perp}\Delta\varepsilon-\frac{4\pi}{\lambda}T_i\,\Delta_v \quad (3)$$

After separating the linear deformation rate and the elevation error, the residual phase is expressed as:

$$\varphi_i^{res}=\varphi_i^{nl}+\varphi_i^{a}+\varphi_i^{n} \quad (4)$$

In the formula, φ_i^{res} is the residual phase; φ_i^{nl} is the nonlinear deformation phase; φ_i^{a} is the atmospheric delay phase; φ_i^{n} is the noise. Perform spatial low-pass filtering and time domain filtering on the residual map to identify the nonlinear deformation phase. The true deformation phase is the sum of the linear deformation and the nonlinear deformation phase:

$$\varphi_{def}=\varphi_l+\varphi_{nl} \quad (5)$$

In the formula, φ_{def} is the total deformation; φ_l is the linear deformation; φ_{nl} is the non-linear variable.

After the Sentinel-1B SLC data format is converted and cropped, the main image is the image on November 2, 2018, and the 5 times critical baseline threshold is used to make other data and the main image establish a master-slave data pair, and then perform an interference workflow to combine all images It is registered to the main image, and 4 times sampling is selected in the distance to avoid the generation of fast-changing interference fringes. Use DEM data to flatten, and then perform radiometric calibration to determine the amplitude dispersion index. The first step is inversion to obtain the displacement rate and residual terrain to flatten the synthesized interferogram. The second step is inversion to estimate and remove the atmospheric phase component to obtain the final deformation rate. After geocoding, the coherence threshold is greater than 0.45 on the surface The deformation result is projected to the vertical direction to make a vertical deformation rate grid graph.

3 Results

In the settlement monitoring calculation results, 87.94% of the PS points have a correlation greater than 0.7. The settlement change value of the SAR image from December 2019 to October 2020 is calculated, and 46 level monitoring points that overlap with the image calculation result patches are selected and used The monitoring value is compared with the patch value for accuracy verification (Figure 1). The verification results show that the maximum difference between the monitoring values obtained by the two monitoring methods is 8.98mm/a, the minimum is 0.04mm/a, the average error is 1.13mm/a, and the root mean square error is 3.09mm/a. Correlation The coefficient is 0.67, and the settlement trends calculated by the two are basically the same, indicating that the settlement results obtained from the SAR images in the area calculated by using the PS-InSAR technology are highly reliable.

Most of the urban surface of Changchun City is stable without changes in subsidence. Most of the urban geological structure is located on the first and second terraces of the Cenozoic Quaternary, and the terraces are stable and not prone to subsidence. Areas with small-scale settlements are located in Jilin Overpass, Century Plaza, Guoxinmeiyi and Ecological Plaza (Figure 2). The maximum settlement rate is 20.45mm/a, and the average settlement rate is 2.98mm/a.

The average settlement rate in the Jilin overpass area is 4.23mm/a, and the cumulative settlement is 16.92mm (Figure 3). Since 2012, three new buildings have been built in this area. Although all of them were completed before 2016, they may also have a certain impact on the regional surface settlement.

The subsidence area of Century Plaza is relatively large and the velocity distribution is uneven. The average settlement rate in the northern region is 11.60mm/a and the

cumulative settlement is 46.41mm. The average settlement rate in the southern region is 8.89mm/a and the cumulative settlement is 35.56mm. The average settlement rate in the eastern region is 6.72mm/a. The cumulative settlement is It is 26.89mm, the average settlement rate in the western region is 1.82mm/a, the cumulative settlement is 7.29mm, the average settlement rate in Zhaojiadian area is 5.83mm/a, and the cumulative settlement is 23.31mm. There are many new buildings in the Century Plaza area, there are many factories, and the settlement is relatively concentrated.

The average settlement rate in Guoxinmeiyi area is 9.37mm/a, and the cumulative settlement is 37.48mm. The geological structure in this area is the structure of the Mesozoic Cretaceous Yaojia Formation. The top of this structure is composed of gray siltstone interbedded, with gravel-bearing medium-coarse sandstone in some parts; brown-red mainly, thick argillaceous rock layer, fine siltstone There are few interlayers and a small amount of calcareous nodules; thin argillaceous siltstone layers are occasionally seen at the bottom. Relative to other structures, the stability is poor. Two earthquakes of magnitude ML1.4 and ML1.3 occurred in the southern part of this area in 2001 and 2006 respectively [15], and geological activities may be relatively frequent.

The average settlement rate in the ecological square area is 4.65mm/a, and the cumulative settlement is 18.59mm. Three new buildings and an elementary school have been built in this area, and expressway construction projects have also been carried out, which may have a certain impact on the surface settlement of the area.

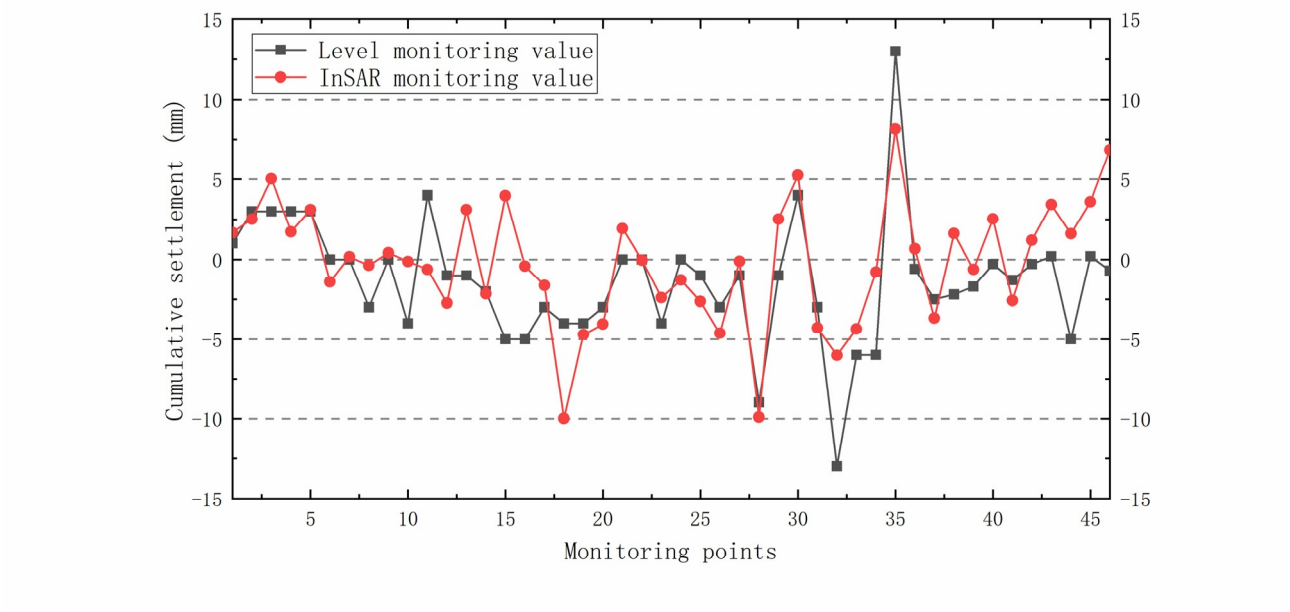

Fig.1. Comparison of InSAR monitoring values and level monitoring values

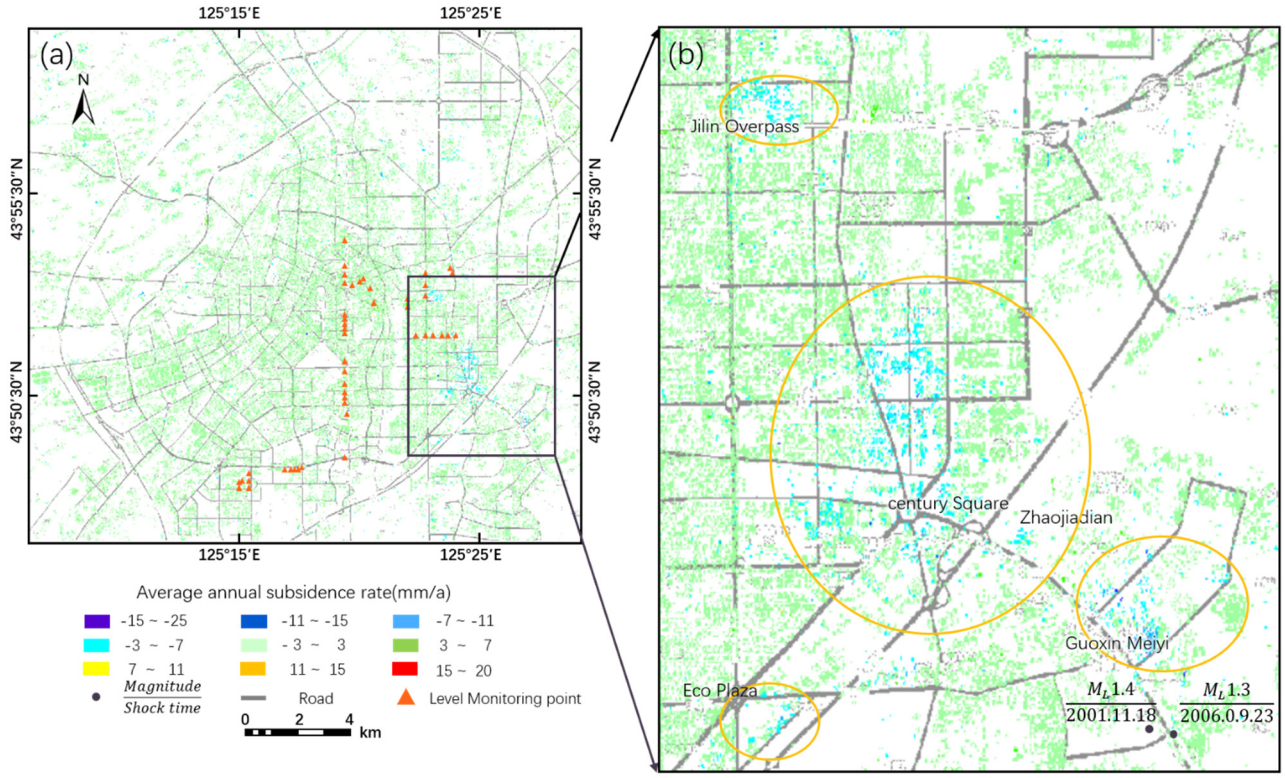

Fig.2. (a) 2016-2020 settlement rate in urban areas of Changchun,(b) Settlement rate in small scale settlement area

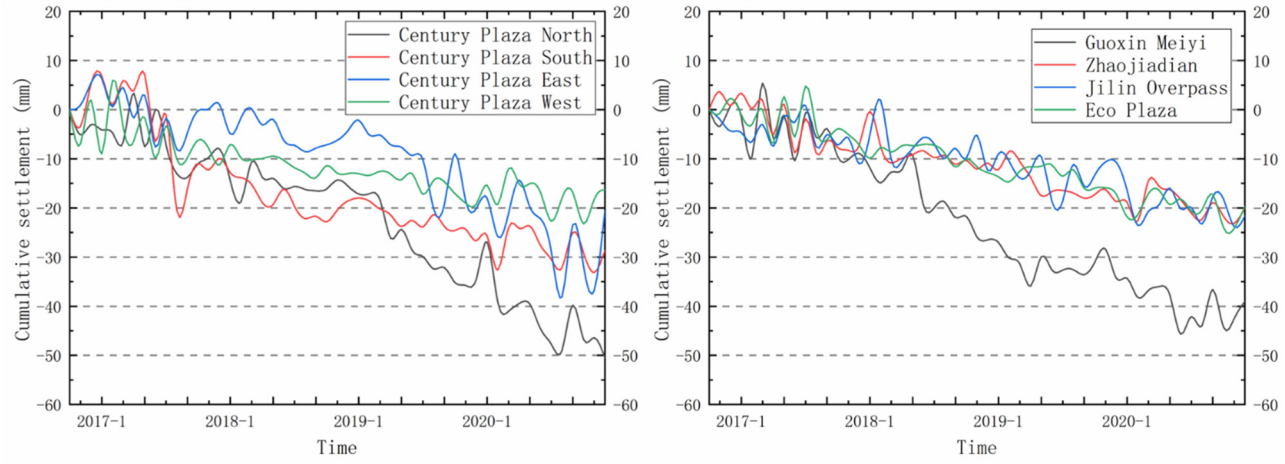

Fig.3. Accumulated settlement in each area

4 Conclusion

(1) Most of the surface of Changchun City is stable without changes in subsidence;

(2) There are four small-scale settlement areas in the southeast of Changchun City: Jilin Overpass, Century Plaza, Guoxinmeiyi and Ecological Plaza;

(3) Engineering construction and unstable geological structure in some areas may be the main cause of settlement in Changchun City.

(4) The key settlement monitoring area of Changchun in the future is the southeast area with Century Square as the centre, and the influence of construction on surface deformation should be minimized.

References

1. Wu Xueyu, Zhao Zhisheng, Bao Ziyu. Research on inversion method of urban land subsidence using SBAS technology [J]. Modern Surveying and Mapping,2019,42(06):9-12.
2. WU Q , JIA C , CHEN S , et al. SBAS-InSAR Based Deformation Detection of Urban Land, Created from Mega-Scale Mountain Excavating and Valley Filling in the Loess Plateau: The Case Study of Yan'an City[J]. Remote Sensing, 2019, 11(14):1673-1683.
3. Ao Meng, Zhang Lu, Liao Mingsheng, Zhang Li, Adaptive fusion deformation measurement of multi-source InSAR data based on variance component estimation [J]. Chinese Journal of Geophysics, 2020, 63(08): 2901-2911.
4. Shi W , Chen G , Meng X , et al. Spatial-Temporal

Evolution of Land Subsidence and Rebound over Xi'an in Western China Revealed by SBAS-InSAR Analysis[J]. Remote Sensing, 2020, 12(22):3756-3776.

5. Lu Yanyan. Land subsidence monitoring and influencing factors analysis based on multi-source SAR data in Su-Xi-Chang area [J]. Acta Geodaetica et Cartographica Sinica, 2019,48(07): Backinsert 1.
6. Chen Qinghua, Bai Guifeng, Chen et al. Study on land subsidence monitoring in Changchun city based on PS-InSAR technology [J]. Geomatics & Spatial Information Technology, 2017, 40(09):185-190.
7. CIAMPOLI L B , GAGLIARDI V, FERRANTE C , et al. Displacement Monitoring in Airport Runways by Persistent Scatterers SAR Interferometry[J]. Remote Sensing, 2020, 12(21):3564-3577.
8. Mo Ying, Zhu Yufeng, Jiang Liming, et al. Land subsidence monitoring based on Sentinel-1A time series InSAR in Nanchang City [J]. Journal of Geodesy and Geodynamics, 2020, 40(03):54-59.
9. CHEN D,CHEN H,WEN Z, et al. Characteristics of the Residual Surface Deformation of Multiple Abandoned Mined-Out Areas Based on a Field Investigation and SBAS-InSAR: A Case Study in Jilin, China[J]. Remote Sensing, 2020, 12(22) : 3752-3752.
10. Dou Chao, Zhao Lijiang, Zhang Shengpeng, et al. Surface Subsidence Monitoring Based on InSAR Data in Golmud City [J]. Bulletin of Surveying and Mapping,2020,(10):123-126.
11. Wang Shengyan, PS_INSAR based monitoring of urban land surface subsidence [J], Geoscience and Spatial Information, 2020,18(9):113-121.
12. Zhou Yuchen, LI Jinping, LU Haojian, et al. Study on land surface subsidence and its mechanism in Changchun city based on SBAS-InSAR [J]. Journal of Heilongjiang Institute of Technology, 2019, 33(03):20-25.
13. You Hong, Mi Hongyan, Zuo Xiaoqing, et al. InSAR based on PS and SBAS for subsidence monitoring in the main urban area of Guiyang [J]. Urban Surveying, 2020,179(04):79-83.
14. Li Lu, Hong Youtang. Study on land subsidence monitoring in Taiyuan based on PS-InSAR technology [J]. Mine Surveying, 2020,208(04):54-59.
15. Zhang Jianwei, Wang Xikui, Sui Weiguo, et al. Seismological and geological tectonic activity analysis in Changchun area [J]. Inland Seismology, 2010, 024(003): 269-274.